PII: S0955-2219(96)00187-2

Fabrication, Characterisation and Formation Mechanism of $Pb_{1.83}Mg_{0.29}Nb_{1.71}O_{6.39}$ Pyrochlore

A. Mergen & W. E. Lee

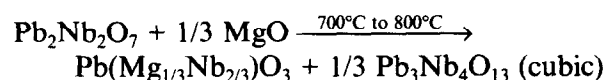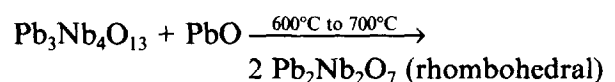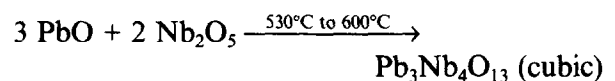University of Sheffield, Department of Engineering Materials, Sheffield S1 3JD, UK

Abstract

$Pb_{1.83}Mg_{0.29}Nb_{1.71}O_{6.39}$ (PMN) pyrochlore ceramics were fabricated from solid state reaction of mixed oxides and by partial oxalate methods. For both methods the pyrochlore crystal structure was not formed directly but via a sequence of intermediate reactions. However, the formation temperature of PMN pyrochlore was lower for the partial oxalate method due to the higher reactivity of these powders. Microstructural investigation of pellets produced from mixed oxides and partial oxalate powders prepared using columbite ($MgNb_2O_6$) revealed only single-phase pyrochlore whereas those produced from partial oxalate powders made using uncalcined Mg and Nb oxides contained clusters of perovskite grains with intergranular Mg-rich phases. Pyrochlore ceramics produced from partial oxalate powders showed higher dielectric constant but lower dielectric loss than those produced from mixed oxides. © 1997 Elsevier Science Limited.

1 Introduction

The family of complex perovskite compounds $Pb(AB)O_3$ (e.g. $A=Mg^{2+}$, Zn^{2+}, Fe^{3+} and $B=Nb^{5+}$ and W^{6+}) are excellent commercial ferroelectric ceramics mainly due to their low firing temperature (~1000°C), which leads to a reduction in the cost of internal electrodes, very high dielectric constant ($K>12000$ at 20°C) and their temperature-insensitive characteristic response (arising from a diffuse phase transition). However, their dielectric properties depend strongly on the purity of the raw materials and method of preparation, since dielectric constant can be affected by second-phase pyrochlore which forms upon processing. Table 1 shows some of these ferroelectric ceramics and the related pyrochlore phases. To obtain the maximum dielectric constant, the pyrochlore phases have to be eliminated from the perovskite microstructure since they are non-ferroelectric and have low dielectric constants.

Lead magnesium niobate, $Pb(Mg_{1/3}Nb_{2/3})O_3$ (PMN) was first fabricated by Smolenskii and Agranovskaya[2] in the late 1950s and is one of the most studied of these complex lead-based perovskites. The main problem with PMN ceramics is the difficulty of fabricating them reproducibly without formation of the stable pyrochlore phase during the initial stages of reaction between the mixed oxides. In producing PMN perovskite ceramics different processing routes can be utilized to minimize the amount of pyrochlore phase formed. These include using (a) finer particle size, purer and more reactive raw materials (such as $MgCO_3$ instead of MgO) and more homogeneous mixing of the starting materials,[3,4] (b) the columbite method which involves precalcination of MgO and Nb_2O_5 to form $MgNb_2O_6$,[5] (c) excess PbO and MgO[6,7] and (d) repeated calcination and milling.[8] All of these techniques decrease the amount of parasite pyrochlore in different ways such as by increasing the reactivity of refractory MgO, by decreasing the PbO loss, and by forming perovskite before formation of pyrochlore which is sluggish in converting to perovskite. Inada,[8] who first proposed a reaction sequence for the formation of PMN, showed that its fabrication from mixed oxides necessarily involves formation of phases in the binary oxide system $PbO–Nb_2O_5$:

$$3\ PbO + 2\ Nb_2O_5 \xrightarrow{\ 530°C\ to\ 600°C\ } Pb_3Nb_4O_{13}\ (cubic)$$

$$Pb_3Nb_4O_{13} + PbO \xrightarrow{\ 600°C\ to\ 700°C\ } 2\ Pb_2Nb_2O_7\ (rhombohedral)$$

$$Pb_2Nb_2O_7 + 1/3\ MgO \xrightarrow{\ 700°C\ to\ 800°C\ } Pb(Mg_{1/3}Nb_{2/3})O_3 + 1/3\ Pb_3Nb_4O_{13}\ (cubic)$$

This reaction sequence suggests that formation of PMN perovskite depends directly on the reactivity

Table 1. Curie temperatures (T_c) and dielectric constants of perovskite ferroelectric ceramics (K_{Pr}) and related pyrochlore phases (K_{Py}). Dielectric constants of the polycrystalline PMN perovskite ceramics were taken from Ling *et al.* (Ref. 1.)

Relaxor material	$T_C(^\circ C)$	K_{Pr}	Pyrochlore phase	K_{Py}
$Pb(Mg_{1/3}Nb_{2/3})O_3$	0 to -15	14600	$Pb_{1.83}Nb_{1.71}Mg_{0.29}O_{6.39}$	130
$Pb(Zn_{1/3}Nb_{2/3})O_3$	140	22000	$Pb_2Nb_{1.4}Zn_{0.6}O_{6.1}$	125
$Pb(Fe_{1/2}Nb_{1/2})O_3$	105	21000	Pb_2FeNbO_6	—
$Pb(Fe_{2/3}W_{1/3})O_3$	-95	10500	$Pb_2FeWO_{6.5}$	65

of MgO with the other phases in the $PbO-Nb_2O_5$ binary system so that methods which improve MgO reactivity also increase the percentage of perovskite phase.

The pyrochlore phase which is formed in PMN perovskite is believed to be a Mg-incorporated $Pb_3Nb_4O_{13}$ cubic pyrochlore. Various compositions have been reported for the PMN pyrochlore. Adrianova *et al.*[9] produced PMN pyrochlore by growing Pb, Mg and Nb oxides from the melt and reported a composition of $Pb_2Mg_{0.32}Nb_{1.87}O_7$. PMN pyrochlore with the formula $Pb_{1.83}Mg_{0.29}Nb_{1.71}O_{6.39}$ was produced by Shrout and Swartz[10] being paraelectric with dielectric constant $K = 130$ at room temperature with an anomalous peak near 20 K due to a relaxation phenomenon. Single-crystal PMN pyrochlore with composition $Pb_{1.86}Mg_{0.24}Nb_{1.76}O_{6.5}$ has also been produced using a PbO flux.[11] Wakiya *et al.*[12] examined the solubility of Mg^{2+} into the Nb^{5+} site along the composition $Pb_{(3+3x)/2}Mg_xNb_{(2-x)}O_{6.5}$ where $0 \le x \le 0.5$ (note that when $x = 0$ the formula gives the $Pb_3Nb_4O_{13}$ cubic pyrochlore) and found that the solubility limit of Mg^{2+} is $x = 0.24$ giving $Pb_{1.86}Mg_{0.24}Nb_{1.76}O_{6.5}$.
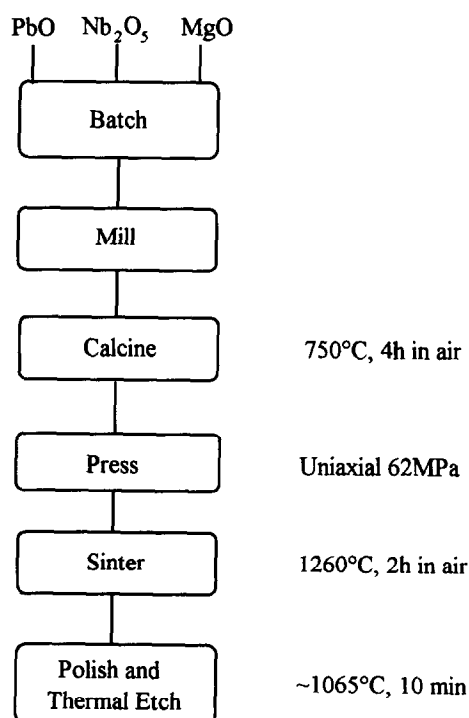
In the present study PMN pyrochlore was produced from solid state reaction of mixed oxide powders and via a simple partial oxalate method with no need for pH control or expensive starting materials. The reaction sequence in both methods has been investigated from extensive differential thermal analysis (DTA) and X-ray diffraction (XRD) analysis starting from the unreacted powders to achieve a better understanding of the perovskite–pyrochlore problem. In addition, the effect of the columbite method on the reaction sequence of PMN pyrochlore was also investigated to understand the success of this approach on producing single-phase PMN perovskite. Unlike all other previous studies the microstructural evolution was examined using detailed electron microscopy. The dielectric properties of PMN pyrochlore were also investigated.

2 Experimental

PMN pyrochlore with the composition $Pb_{1.83}$-$Mg_{0.29}Nb_{1.71}O_{6.39}$ as determined by Shrout and

Swartz[10] was produced using mixed oxides and partial oxalate methods. The partial oxalate method gives improved mixing and has been successfully used for preparation of lead-based electro-optic materials such as PZT (lead zirconate titanate), PLZT (lanthanum modified PZT)[13] and also for fabrication of PMN (lead magnesium niobate) relaxor ferroelectrics.[14] In the mixed oxide method, yellow lead oxide (PbO, >99.9%), niobium oxide (Nb_2O_5, >99.5%) and magnesium oxide (MgO, >99%) powders (all from Aldrich Chemical Company Ltd, Gillingham, Dorset, UK) were wet ball milled in ethanol for 4 h using zirconia balls. Figure 1 shows a block diagram of the mixed oxide route. The milled powder slurry was dried at 120°C for 24 h.

PMN pyrochlore was also produced by a partial oxalate method using two different approaches. The flow chart of the main steps of this process can be seen in Fig. 2. In the first approach, reagent-grade starting powders of Nb_2O_5 and MgO, used also in the mixed oxide method, were milled in ethanol for 1 h with zirconia balls. The slurry was dried at 120°C for 24 h and calcined at 1100°C for 5 h to produce

PbO Nb_2O_5 MgO

Batch

Mill

Calcine — 750°C, 4h in air

Press — Uniaxial 62MPa

Sinter — 1260°C, 2h in air

Polish and Thermal Etch — ~1065°C, 10 min

Fig. 1. Processing of PMN pyrochlore via the mixed oxides method.

columbite ($MgNb_2O_6$). The resulting calcined powders were ground in ethanol for 1 h using zirconia balls and dried at 120°C overnight. However, in the second approach Nb_2O_5 and $(MgCO_3)_4.Mg(OH)_2.5H_2O$ powders were ball milled in ethanol for 1 h using zirconia balls and dried at 120°C for 24 h. Hereafter the first approach will be designated by CMN, calcined MgO and Nb_2O_5, and the second approach will be designated by UCMN, uncalcined MgO and Nb_2O_5. Both dried powders, CMN and UCMN powders, were dispersed in 2 M oxalic acid solution and stirred for 2 h. The lead solution was prepared by dissolving $Pb(NO_3)_2$ in distilled water and adding dropwise to the oxalic acid $((COOH)_2.2H_2O)$–water solution. In both cases lead precipitates as lead oxalate and coats the

CMN and UCMN powders giving a homogenous mixture.[13] These precipitates were washed several times with distilled water in the first approach while in the second approach the solution was evaporated to dryness at 120°C since MgO dissolves in the oxalic acid.[14] Therefore in UCMN lead oxalate only coats the dispersed niobium oxide particles since magnesium remains in the solution. When the solution is evaporated to dryness the magnesium oxide recovered remains uncoated which may lessen the benefit of this route. In both cases the dried powders were mixed in ethanol for 1 h. Dried powders produced from mixed oxide and partial oxalate methods were then calcined in a closed alumina crucible at 750°C for 4 h. Calcined CMN and UCMN powders were further milled in ethanol for 1 h.

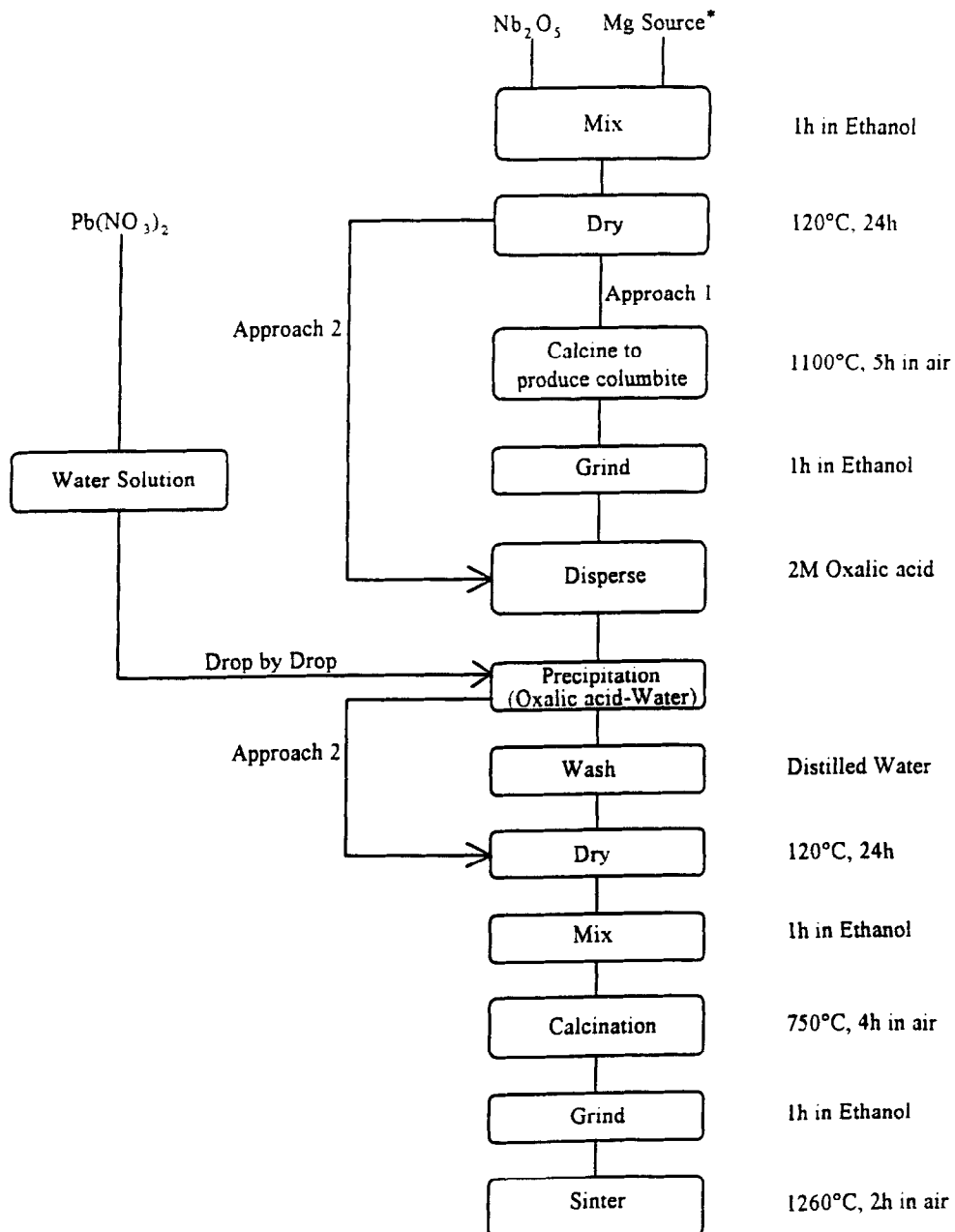Fig. 2. Processing route to PMN pyrochlore from the partial oxalate method. In approach 1 MgO and Nb_2O_5 were calcined to produce columbite ($MgNb_2O_6$) whereas in approach 2 hydromagnesite and niobium oxide were directly used without calcination. (*MgO for CMN and $(MgCO_3)_4.Mg(OH_2).5H_2O$ for UCMN).

Pellets pressed at 62 MPa and made from unreacted powders heated at a rate of 300 K/h and air-quenched at 50°C intervals between 350°C and 1100°C were used to determine the possible reaction sequences during single-phase pyrochlore formation in both mixed oxide and partial oxalate methods. In addition, the phase development in dried but uncalcined powders was examined using differential thermal analysis (DTA) and thermogravimetric analysis (TGA) at a heating rate of 10 K/min in air. The resultant powders and heat-treated pellets were then analysed by X-ray diffraction (XRD) with a Philips diffractometer using Cu K_α radiation from 10 to 85° 2θ at a speed of 1°/min. The particle sizes and the extent of the agglomeration in the starting oxides were estimated using SEM (Jeol 6400). The lattice parameter of the pyrochlore was determined using a least squares method and an internal gold standard over a high angle region and at a low speed of 0·25°/min. Table 2 gives crystallographic information about phases observed in this study.

Pellets uniaxially pressed at 62 MPa made from calcined powders were fired between 700 and 1260°C for 2 h at heating and cooling rates of 300 K/h. The amount of perovskite or pyrochlore phase at the sintering temperature was calculated using the following equation:[5]

$$Py\% = 100 \times \frac{I_{py}}{(I_{pr} + I_{py})}$$

or $$Pr\% = 100 \times \frac{I_{pr}}{(I_{pr} + I_{py})} \quad (1)$$

where Py% and Pr% are the volume percentage of pyrochlore and perovskite phases, I_{pr} refers to the (110) perovskite peak and I_{py} refers to the (222) pyrochlore peak. Bulk densities of the pellets were measured with a mercury densitometer and theoretical density was calculated using XRD results. Sintered pellet microstructures were examined using SEM (Jeol 6400) and TEM (Jeol 200CX operated at 200 kV). SEM samples were thermally etched at ~1060°C in air for about 10 min. TEM samples were prepared using standard ceramographic techniques and Ar ion-beam thinning.

Grain size distributions were measured using a linear intercept technique[15] on secondary electron images of polished and etched samples. Energy Dispersive Spectroscopy (EDS) was performed using LINK AN10000 and eXL systems on the SEM and TEM (Philips 420T operated at 120 kV). Samples for dielectric measurements were prepared from pellets, sintered at 1260°C for 2 h, by polishing the faces flat and parallel and by firing on silver electrodes (Dupont 7095) at 550°C for 30 min. Dielectric measurements were performed at the Department of Metallurgy and Materials Science, University of Manchester, using a HP4284A precision LCR meter.

3 Results and Discussion

3.1 Powder characterization

XRD analysis of uncalcined CMN powders revealed only columbite and lead oxalate indicating that the added niobium and magnesium oxides reacted mostly to form $MgNb_2O_6$. SEM of the starting oxides revealed that PbO particles are plate-like with 2–7 μm average size. Nb_2O_5 powders have a sub-micrometre ultimate particle size although occurring in 10–20 μm agglomerates while the MgO powder is flake-like with 1–5 μm average size.

Figure 3 shows DTA of the mixed oxides of $PbO–MgO–Nb_2O_5$ at an atomic ratio of 1·83:0·29: 0·855 prepared via solid state reaction. The exothermic peak at approximately 400°C is thought to be due to transformation of orthorhombic PbO (yellow) to tetragonal PbO (red). XRD of quenched samples made from unreacted powders showed that PbO (red) starts to form above 400°C. Lead monoxide occurs in two polymorphic forms.[16] The orthorhombic, β-form called massicot, is yellow and stable at elevated temperatures and the tetragonal, α-form called litharge, is red and stable up to 490°C. At room temperature the yellow PbO is metastable and may transform to the stable red PbO on grinding.[16] However, in mixed oxide PMN pyrochlore powder, yellow PbO remained metastable after milling and started to transform to red PbO only above 400°C. In addition, at high

Table 2. Phases found throughout this study with their crystal system, lattice parameter, space group and JCPDS card number

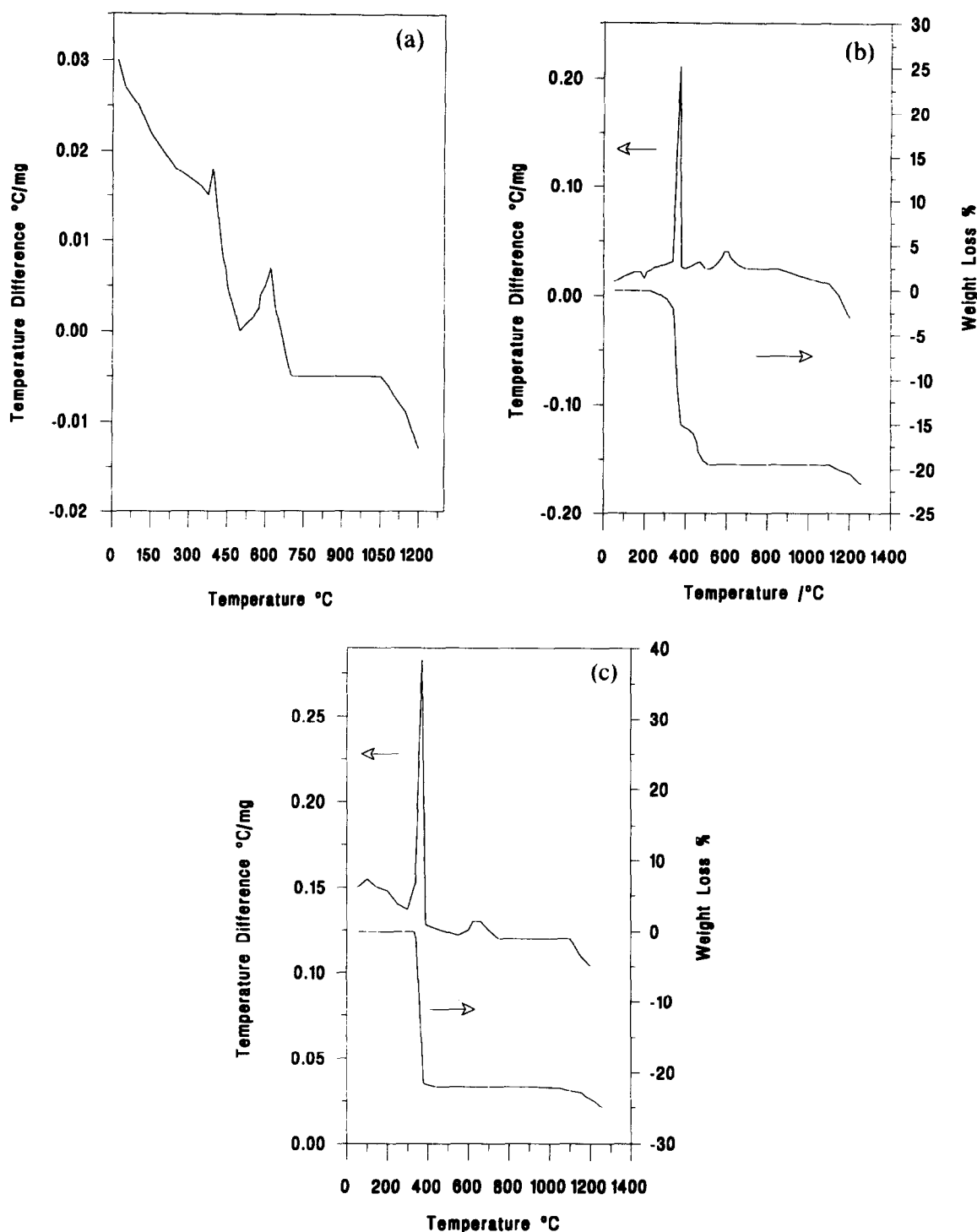| Phase	Structure	Lattice parameter (Å)	Space group	JCPDS card
$Pb_3Nb_4O_{13}$	Cubic	a = 10·56	Fd3m (227)	25–443
$Pb_2Nb_2O_7$	Rhombohedral	a = 10·67 α = 84°73'	—	16–175
$PbMg_{1/3}Nb_{2/3}O_3$	Cubic	a = 4·049	Pm3M (221)	27–1199
$Mg_4Nb_2O_9$	Hexagonal	a = 5·1616 c = 14·0218	—	36–1381
$Pb_{1·83}Mg_{0·29}Nb_{1·71}O_{6·39}$	Cubic	a = 10·601	Fd3m (227)	37–71

Fig. 3. Thermogravimetric and differential thermal analysis of (a) mixed oxide (DTA only), (b) UCMN and (c) CMN powders having a ratio of $PbO:MgO:Nb_2O_5 = 1.83:0.29:0.855$.

temperatures, around 700°C, yellow PbO again started to form by transformation of red PbO. The other exothermic peak at 600–650°C was examined by performing XRD on samples heated to temperatures either side of each peak using identical conditions as for the thermal analyses. This peak was from formation of cubic pyrochlore with the formula 3 $PbO.2$ Nb_2O_5 ($Pb_3Nb_4O_{13}$). The same exothermic peak was also observed by Bouquin and Lejeune[17] for $Pb_3Nb_4O_{13}$ pyrochlore between 500 and 600°C during formation of PMN perovskite. Inada,[8] Imota and Ilda[18] and Kassar-

jian *et al.*[19] also reported the formation of this compound during the reaction sequence for formation of $Pb(Mg_{1/3}$-$Nb_{2/3})O_3$ perovskite.

Figures 3(b) and (c) show TG-DTA curves of the UCMN and CMN respectively. In Fig. 3(b) the small endothermic peak at approximately 200°C is thought to be due to melting of the oxalic acid present since it has a melting point of around 189°C.[20] The large exothermic peak at around 375°C was due to the decomposition of lead oxalate by the following reaction[20,21] since ~15% of weight loss was observed around this

temperature. This was also confirmed by XRD taken from both sides of the peak.

$$PbC_2O_4 \longrightarrow PbO + CO + CO_2$$

Another smaller exotherm was also observed at around 470°C and was considered to be due to the oxidation of lead since the weight loss continued until 500°C (with a total weight loss of ~20%). XRD taken before the 470°C peak but after the major lead oxalate decomposition peak (375°C) showed remnant lead oxalate, indicating that the 470°C peak may be due to oxidation of remaining carbon. The last exotherm between 600 and 700°C was due to formation of $Pb_3Nb_4O_{13}$ cubic pyrochlore as in the mixed oxide powder.

In Fig. 3(c) TG-DTA curves of lead-oxalate-coated $MgNb_2O_6$ powder can be seen. The endothermic peak found in UCMN at around 200°C

was not observed here since this powder was washed several times with distilled water by centrifuge to remove any oxalic acid left from precipitation. Only two exothermic peaks were seen in CMN. The first at approximately 370°C was due to the decomposition of lead oxalate as observed in UCMN (Fig. 3(b)). At this temperature TG revealed around 22% weight loss indicating that carbon is burning. The second exotherm between 600 and 700°C is associated with formation of $Pb_3Nb_4O_{13}$ pyrochlore compound as was the case for UCMN and mixed oxide powders (Figs 3(a) and (b)).

3.2 Reaction sequence

XRD of pellets made from unreacted mixed oxide powders (Fig. 4(a)) revealed no reaction between oxides until 650°C except for initial transformation
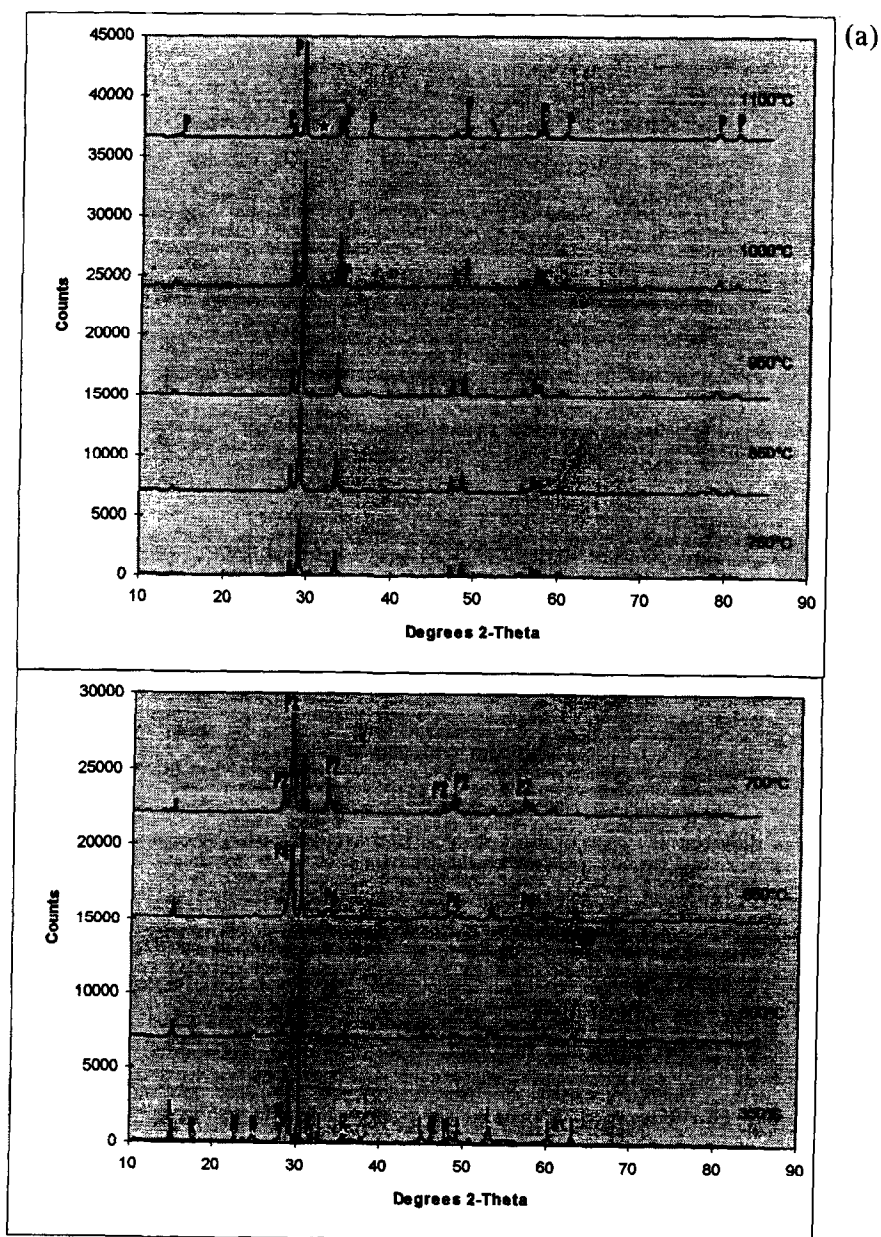
Fig. 4. XRD analysis of powders made from crushed pellets derived from (a) mixed oxide, (b) UCMN and (c) CMN methods and air-quenched from different temperatures to determine possible reaction sequences. R = Red PbO, L = Yellow PbO, N = Nb_2O_5, P4 = $Pb_3Nb_4O_{13}$, P2 = $Pb_2Nb_2O_7$, P = PMN Pyrochlore, * = PMN Perovskite, M = MgO, O = Lead oxalate, C = $MgNb_2O_6$.

of some orthorhombic PbO (yellow) to tetragonal PbO (red) above 400°C (indicated by Fig. 3(a)). At ~650°C 3 PbO.2 Nb_2O_5 ($Pb_3Nb_4O_{13}$) cubic pyrochlore started to form. The formation of this compound produced the exothermic DTA peak at temperatures of between 600 and 650°C (Fig. 3(a)). At higher temperatures, ~700°C, cubic $Pb_3Nb_4O_{13}$ pyrochlore transforms to $Pb_2Nb_2O_7$ rhombohedral pyrochlore, by taking up PbO. In addition, at approximately 600–700°C, the red PbO started to transform to the yellow, high-temperature form of PbO. The amount of $Pb_2Nb_2O_7$ pyrochlore increases with temperature but PbO decreases. As illustrated by XRD of the mixed oxide pellet made from unreacted powders and quenched from 750°C (Fig. 4(a)) the intensity of the PbO peaks is decreased to a low level above this temperature indicating that most of the PbO

reacted to form $Pb_2Nb_2O_7$ pyrochlore around 750°C. Moreover, above 800°C a small amount of $PbMg_{1/3}Nb_{2/3}O_3$ perovskite phase was also seen. Subsequently, at around 1000°C, PMN pyrochlore (cubic) starts to form from rhombohedral pyrochlore and unreacted MgO. The probable reaction sequence in the mixed oxide can be written as follows:
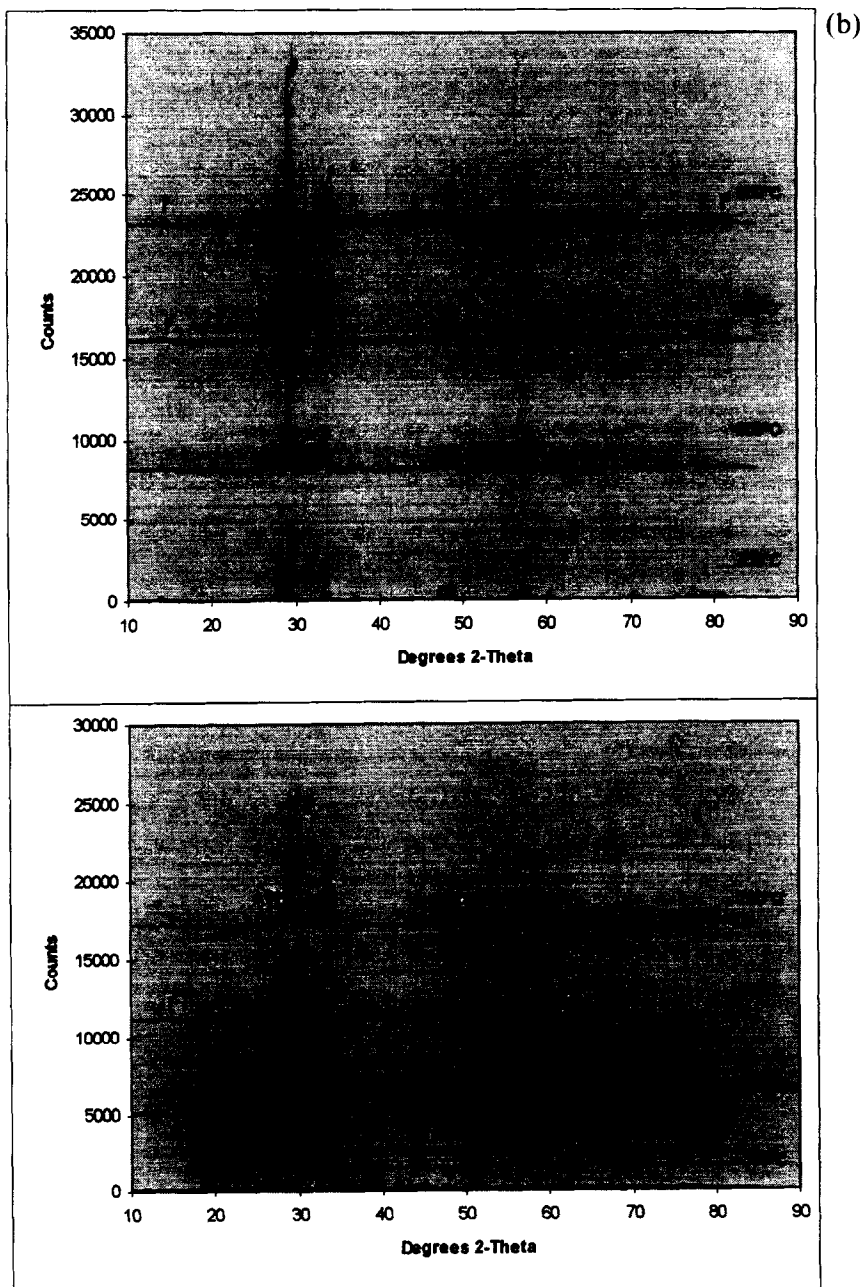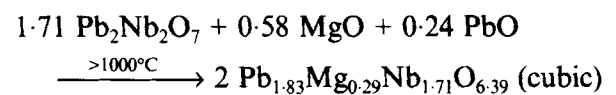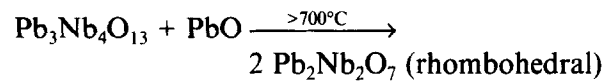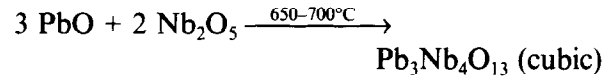
$$3\ PbO + 2\ Nb_2O_5 \xrightarrow{\ 650-700°C\ } Pb_3Nb_4O_{13}\ (cubic)$$

$$Pb_3Nb_4O_{13} + PbO \xrightarrow{\ >700°C\ } 2\ Pb_2Nb_2O_7\ (rhombohedral)$$

$$1\cdot 71\ Pb_2Nb_2O_7 + 0\cdot 58\ MgO + 0\cdot 24\ PbO$$
$$\xrightarrow{\ >1000°C\ } 2\ Pb_{1.83}Mg_{0.29}Nb_{1.71}O_{6.39}\ (cubic)$$

Fig. 4. *Contd.*

Note that although PbO content decreased to a low level above 750°C and XRD indicated no PbO at high temperatures (1000°C for mixed oxide and 800°C for UCMN and CMN), it is written in the last equation to balance it.

The same reaction sequence but at different temperatures was also observed in UCMN. Figure 4(b) shows the XRD of crushed pellets made from unreacted UCMN powders and quenched from temperatures of between 350 and 1000°C. In UCMN after 400°C decomposition of lead oxalate to lead oxide started and tetragonal PbO (red) formed directly. Decomposition of lead oxalate produced two exothermic peaks in DTA, 375°C and 470°C (Fig. 3(b)). After 650°C, $Pb_3Nb_4O_{13}$ cubic pyrochlore started to form. The formation of this compound gave an exothermic DTA peak at temperatures of between 600 and 700°C

(Fig. 3(b)). In addition, at about the same temperature PbO (red) began to transform to PbO (yellow) as observed for the mixed oxides. Above 700°C, further reaction of $Pb_3Nb_4O_{13}$ pyrochlore with PbO led to a rhombohedral pyrochlore $Pb_2Nb_2O_7$. As was observed in the mixed oxide most of the PbO was consumed around 750°C forming $Pb_2Nb_2O_7$. Finally, above 800°C PMN pyrochlore started to form by reaction of $Pb_2Nb_2O_7$ with MgO. It can be clearly seen from Fig. 4(b), above 800°C, that as the temperature increased the amount of PMN pyrochlore increased with a corresponding decrease in the amount of rhombohedral pyrochlore, $Pb_2Nb_2O_7$. However, at around 800°C the (110) peak of PMN perovskite at 31·2° 2θ, which has the strongest intensity, was detected but disappeared after 950°C possibly due to reaction with MgO

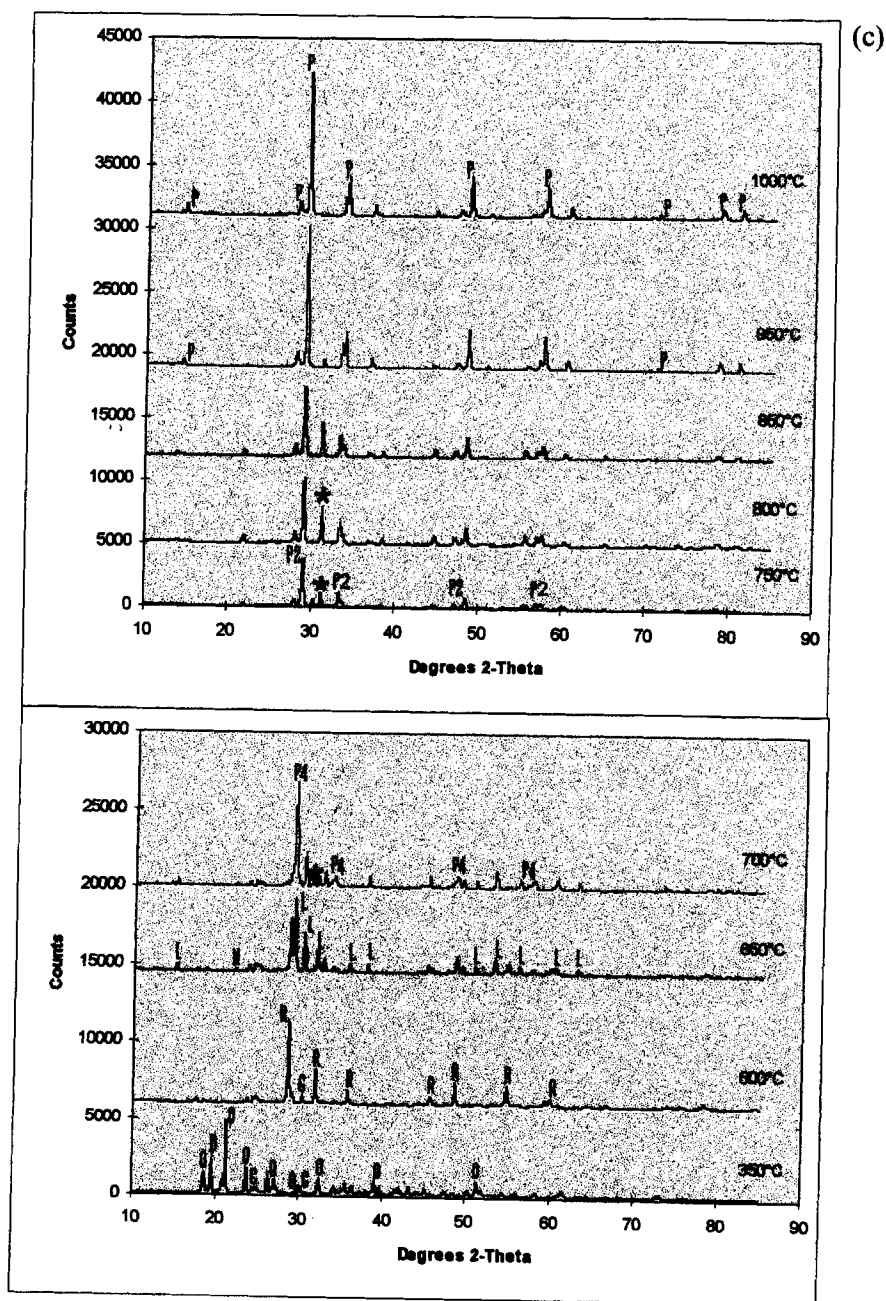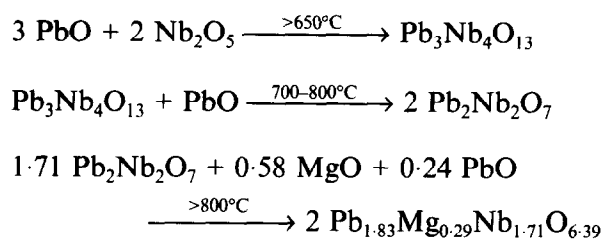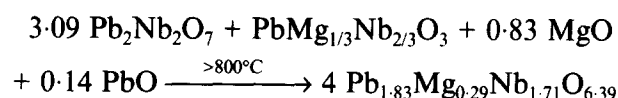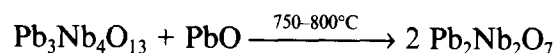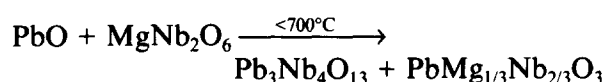Fig. 4. Contd.

forming the pyrochlore. In the UCMN method the PMN pyrochlore did not form directly but by the following reactions as in the mixed oxide route:

$$3\ PbO + 2\ Nb_2O_5 \xrightarrow{\ >650°C\ } Pb_3Nb_4O_{13}$$

$$Pb_3Nb_4O_{13} + PbO \xrightarrow{\ 700-800°C\ } 2\ Pb_2Nb_2O_7$$

$$1.71\ Pb_2Nb_2O_7 + 0.58\ MgO + 0.24\ PbO$$
$$\xrightarrow{\ >800°C\ } 2\ Pb_{1.83}Mg_{0.29}Nb_{1.71}O_{6.39}$$

However, although the formation temperatures of $Pb_3Nb_4O_{13}$ and $Pb_2Nb_2O_7$ pyrochlores were similar in the UCMN and mixed oxide methods the formation temperature of PMN pyrochlore was lower in UCMN. This may be due to the higher reactivity of these powders since the lead oxalate precipitates were submicron in size and more uniform in shape.[22] Nevertheless, in both methods a small amount of perovskite phase also formed along with pyrochlore at high temperatures. The formation of this phase may be attributed to the solubility of hydromagnesite (starting reagent) in the oxalic acid in UCMN and inhomogeneous mixing of the mixed oxide powders. In UCMN since magnesium remains in the solution the lead oxalate only coats the niobium oxide particles and this renders this UCMN method basically the same as the mixed oxide method with the resulting inhomogeneous powders (Section 2).

The reaction sequence in CMN (Fig. 4(c)) was not the same as the others although it involves the formation of lead niobate pyrochlores. Above 400°C lead oxalate starts to decompose giving an exothermic peak at around 370°C (Fig. 3(c)). Decomposition of lead oxalate led to direct formation of PbO (red) as observed in UCMN and the red PbO began to transform to yellow PbO as before. The formation of $Pb_3Nb_4O_{13}$ cubic pyrochlore started above 700°C and it began to transform to $Pb_2Nb_2O_7$ rhombohedral pyrochlore by taking in the lead oxide at around 750°C. Moreover, above 700°C the amount of PMN perovskite formed increased until 800°C, where formation of PMN pyrochlore started. Above 800°C the amount of PMN perovskite and $Pb_2Nb_2O_7$ pyrochlore phases started to decrease by decomposing to PMN pyrochlore. PMN perovskite decreased to a low level by approximately 1000°C. As a result the PMN pyrochlore is not formed directly from the oxides, but through some intermediate compounds involving the lead–niobate pyrochlores and PMN perovskite:

$$PbO + MgNb_2O_6 \xrightarrow{\ <700°C\ }$$
$$Pb_3Nb_4O_{13} + PbMg_{1/3}Nb_{2/3}O_3$$

$$Pb_3Nb_4O_{13} + PbO \xrightarrow{\ 750-800°C\ } 2\ Pb_2Nb_2O_7$$

$$3.09\ Pb_2Nb_2O_7 + PbMg_{1/3}Nb_{2/3}O_3 + 0.83\ MgO$$
$$+ 0.14\ PbO \xrightarrow{\ >800°C\ } 4\ Pb_{1.83}Mg_{0.29}Nb_{1.71}O_{6.39}$$

The columbite method was developed[5] to obtain pyrochlore-free PMN perovskite and, to achieve this aim, MgO and Nb_2O_5 were precalcined to reduce the reaction rate between PbO and Nb_2O_5 forming pyrochlore. In addition, in this method refractory MgO is dispersed essentially on an atomic scale. Using the CMN method the formation temperatures of $Pb_3Nb_4O_{13}$ cubic pyrochlore and $Pb_2Nb_2O_7$ rhombohedral pyrochlore were higher than in the UCMN and mixed oxide routes. This is considered to be due to the PbO which cannot liberate the Nb_2O_5 from columbite at low temperatures. In other words the kinetics of this reaction appear to be slow enough to prevent pyrochlore formation.[5] In addition, formation of $PbMg_{1/3}Nb_{2/3}O_3$ perovskite was also observed before formation of PMN pyrochlore in CMN after 700°C. From these results it can be concluded that the columbite route is an effective way of producing a single-phase perovskite ceramic since it causes direct PMN perovskite formation before PMN pyrochlore and, since the process of transforming pyrochlore into perovskite is sluggish,[5,23] the formation of PMN perovskite before pyrochlore is preferred.

In summary, it can be concluded that in both mixed oxide and partial oxalate methods the pyrochlore PMN was formed not by the direct formation of oxides but through the formation of some complex sequence of intermediate compounds. In the PbO–Nb_2O_5–MgO system the phase evolution up to 700°C in CMN, 800°C in UCMN and up to 950°C in the mixed oxide is similar to the PbO–Nb_2O_5 system.[19,24] As the XRD analysis (Fig. 4) indicates, PbO reactivity for all methods is greatly increased above 750°C. Similar results have also been reported for other PbO-containing systems such as PbO–TiO_2–ZrO_2.[25] In all three methods the formation temperature of PMN pyrochlore was high, particularly in the mixed oxide, because of the poor reactivity of refractory MgO.[3,7]

It appears that the formation of PMN pyrochlore is very dependent on the reactivity of MgO as in the formation of the PMN perovskite phase[4,5,8] since the poor dispersion and/or the refractory nature of MgO particles allows PbO and Nb_2O_5 particles to react preferentially to form the lead niobate pyrochlore phases.

The above section has discussed in detail fabrication of PMN pyrochlore from different routes
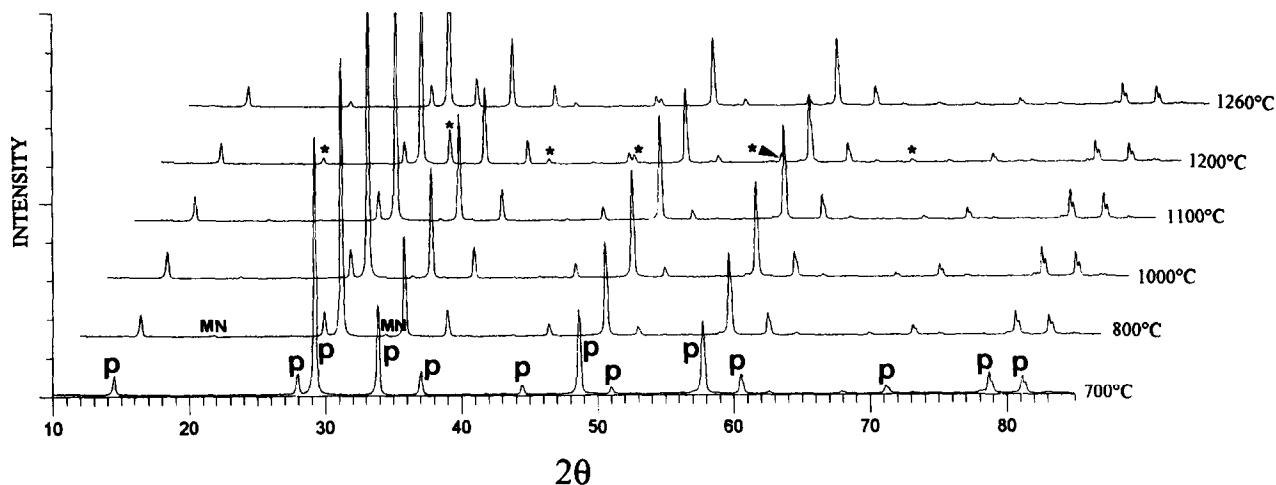
Fig. 5. XRD analysis of crushed pellets held at different temperatures for 2 h made from calcined powders and derived from UCMN to determine the phase development in calcined PMN pyrochlore powder. P = PMN Pyrochlore, MN = $Mg_4Nb_2O_9$, * = PMN Perovskite.

and their reaction sequence and phase analysis during formation of pyrochlore. The following section will discuss the detailed characterization of calcined powder and pyrochlore ceramics including XRD, density, microstructures and dielectric properties.

3.3 Detailed characterization of the PMN pyrochlore

Although XRD of crushed, sintered pellets, fired 2 h at 1260°C, made from mixed oxide and CMN methods only indicated single-phase pyrochlore, XRD of sintered UCMN pellet revealed PMN perovskite in addition to pyrochlore (Fig. 5). It was found that after sintering 2 h at 1260°C there was around 87% of pyrochlore and 13% of perovskite. In addition, phase development in calcined UCMN pellets fired between 700 and 1260°C for 2 h followed using XRD (Fig. 5) revealed that above 800°C a small amount of magnesium niobium compound, $Mg_4Nb_2O_9$, also formed and disappeared above 1100°C where formation of $PbMg_{1/3}Nb_{2/3}O_3$ perovskite phase started. The formation of these compounds is thought to be due to the inhomogeneous distribution of MgO within the UCMN microstructure as explained in Section 3.2. This inhomogeneous distribution of MgO in the microstructure leads to formation of the $Mg_4Nb_2O_9$ compound and finally formation of PMN perovskite. As observed from the reaction sequence study the formation of both PMN pyrochlore and perovskite is directly related to the reactivity of the refractory MgO. Therefore the homogeneous dispersion of MgO is a critical factor and inhomogeneous dispersion of MgO may easily cause PMN perovskite formation in the PMN pyrochlore because the perovskite ($PbMg_{1/3}$-$Nb_{2/3}O_3$) has higher MgO content than pyrochlore ($Pb_{1.83}Mg_{0.29}Nb_{1.71}O_{6.39}$).

XRD analysis of crushed sintered pellet made from mixed oxides indicated that the $Pb_{1.83}Mg_{0.29}$-$Nb_{1.71}O_{6.39}$ composition was a cubic pyrochlore structure type (space group Fd3m) with a lattice parameter of a = 10·601±0·001 Å. This value is in good agreement with a = 10·599 Å measured by Shrout and Swartz.[10]

Pellet densities after holding 2 h at temperatures of between 700 and 1260°C are given in Fig. 6. Densities of the samples prepared from partial oxalate methods are higher since the starting powders are more uniform with good physical contact (packing) between particles. This will decrease the diffusion path and lead to dense material at lower temperatures. In addition, larger agglomerates in the calcined mixed oxide powder[22]
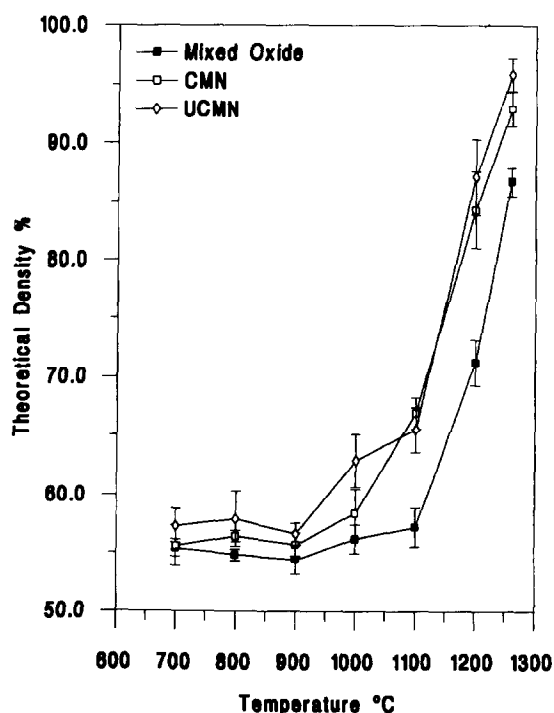

Fig. 6. Relative densities of mixed oxide, UCMN and CMN pellets held for 2 h at temperature.

could also cause low density in pellets produced from this route. Pellets produced from the columbite route, CMN, had generally lower densities than UCMN. This might be due to larger columbite crystals in the starting materials. In both mixed oxide and partial oxalate methods there was a sharp increase in density after 1100°C which could be due to formation of a liquid since there was an endothermic shift from the base line above ~1100°C in all the DTA curves (Fig. 3). At the final sintering temperature, 1260°C for 2 h, the highest theoretical densities observed were ~95% (UCMN), ~93% (CMN) and ~87% (mixed oxide).

SEM micrographs of pellets produced from mixed oxide, UCMN and CMN are shown in Fig. 7. The microstructures of the sintered mixed oxide and CMN pellets were more uniform than that of UCMN pellets due to the inhomogeneous
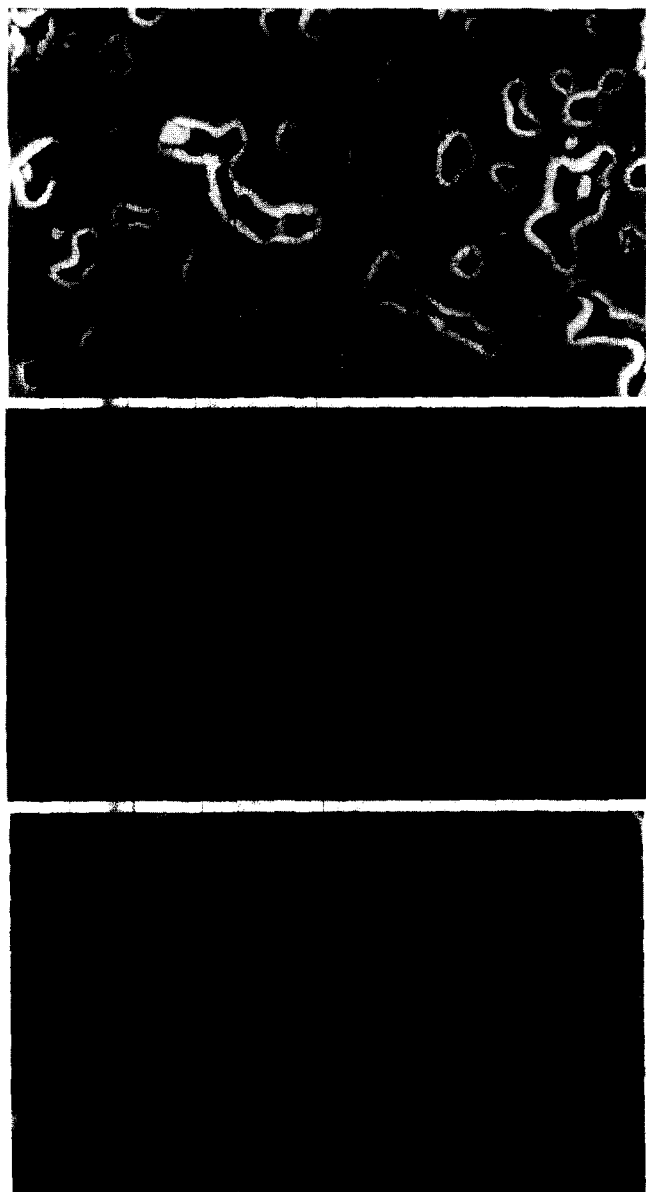
MgO distribution in UCMN after precipitation (Section 3.2). Grain sizes were 8±2 μm, 4±4 μm and 7±3 μm for mixed oxide, UCMN and CMN pellets respectively. PMN perovskite phase formed locally in the PMN pyrochlore produced from UCMN (Fig. 8). Perovskite grains were fine with a grain size of less than 1 μm. EDS analysis reveals that the phases can be differentiated by their Mg content. The perovskite Mg content is higher than that of pyrochlore, calculated as ~2·5 wt% for $Pb(Mg_{1/3}Nb_{2/3})O_3$ perovskite and ~1·09 wt% for $Pb_{1.83}Mg_{0.29}Nb_{1.71}O_{6.39}$ pyrochlore. In addition to perovskite another phase was observed within the UCMN pellet. This phase was only observed between perovskite grains and was absent within pyrochlore grains (Fig. 9). EDS analysis of this phase indicated high magnesium content and due to its low mean atomic number this phase appeared dark in backscattered electron images much like pores, which made it difficult to differentiate from them. Since the XRD analysis (Fig. 5) of fired pellets made from calcined powders revealed $Mg_4Nb_2O_9$ was present until 1200°C, it was thought that this was the same

Fig. 7. Secondary electron SEM images of sintered (a) mixed oxide, (b) UCMN and (c) CMN pellets after 2 h at 1260°C showing smaller grain size (4±4 μm) in UCMN and larger grain size (8±2 μm) in mixed oxide pellets.
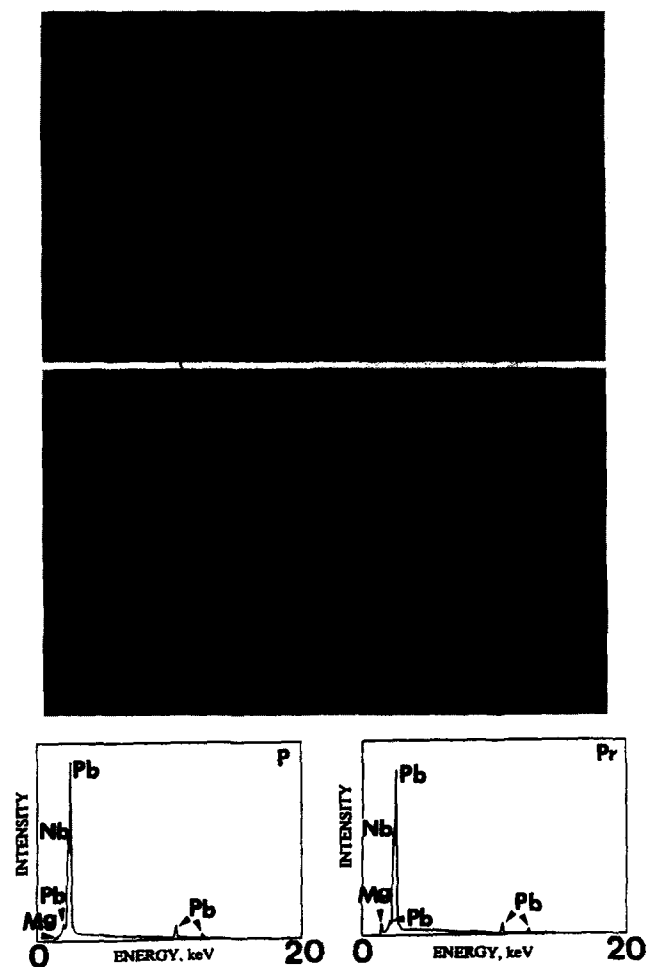

Fig. 8. Secondary electron image of UCMN pellet sintered for 2 h at 1260°C indicating PMN perovskite and pyrochlore phases together with EDS analysis showing the higher concentration of Mg in PMN perovskite. P–Pyrochlore and Pr–Perovskite.

magnesium–niobium compound, which had not transformed. However, evidence of Pb is also found in the EDS spectrum taken from one of these Mg-rich phases (Fig. 9) although this may
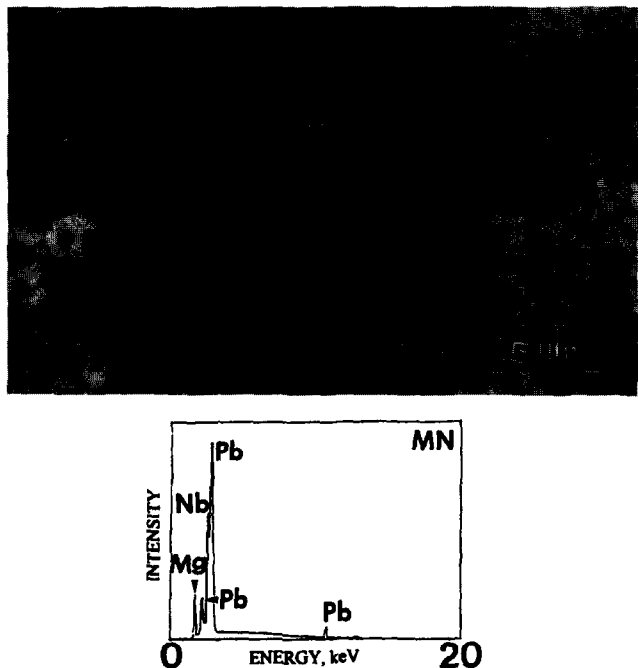

Fig. 9. Backscattered electron image of UCMN pellet after 2 h at 1260°C showing the three phases together: the major PMN pyrochlore phase (P), PMN perovskite (Pr) and minor Mg–Nb phase (MN) with EDS analysis from MN.

be attributed to beam spreading, i.e. it could come from the surrounding perovskite grains or from solid solution of Pb with this Mg–Nb phase. Mg-rich phases have also been observed by others in PMN perovskite.[26,27] In PbO–MgO–Nb$_2$O$_5$ ceramics near the Pb(Mg$_{1/3}$Nb$_{2/3}$)O$_3$ stoichiometric composition prepared by Yan et. al.[28] some Mg-rich second phase was also observed and the presence of this phase was attributed to lead oxide loss by vaporization on sintering.

While SEM images of dense pellets produced from mixed oxides indicated only single-phase pyrochlore, TEM revealed occasional crystalline second phases at grain junctions (Fig. 10(a)). Nevertheless, the grain boundaries were clean and no glassy phase was apparent (Fig. 10(b)). Dislocations were observed at grain boundaries implying the absence of glass there.[29] TEM investigation of pellets produced from CMN and UCMN also revealed the absence of glassy phase at grain boundaries. Figure 11(a) reveals clean grain boundaries between pyrochlore and PMN perovskite grains in UCMN pellets. In Fig. 11(b) the typical shape of faceted perovskite grains observed in UCMN pellets can be clearly seen. Figure 12 shows clean grain junctions in a CMN pellet. Some planar defects[30] were also observed in the pellets produced from mixed oxides, UCMN

Fig. 10. Bright-field (BF) TEM micrographs of mixed oxide pellet sintered at 1260°C for 2 h indicating (a) crystalline second phase at grain junction (S) and (b) grain structure and clean grain boundaries.

Fig. 11. TEM micrograph of UCMN pellet after 2 h at 1260°C demonstrating (a) clean grain boundaries between the PMN pyrochlore (P) and perovskite (Pr) grains, and (b) grain morphologies of PMN perovskite grains.

and CMN (Fig. 13). When the defect labelled A in Fig. 13 was tilted to different reflections to elucidate its nature the contrast was consistent with it being a low-angle grain boundary.[22]

The dielectric properties of PMN pyrochlore were measured between 20 and 120°C at 100 kHz (Figs 14(a) and (b)). In all three pellets dielectric constant significantly and linearly changes as the temperature is raised. The magnitude of dielectric constant decreases from 130 to 110 for the mixed oxide pellet (PMN), from 157 to 134 for CMN and from 286 to 218 for UCMN as the temperature increases from 20 to 120°C. The highest dielectric constant value is observed for the UCMN and this is due to the PMN perovskite phase formed in the microstructure (13 vol% perovskite). Although the dielectric constants of PMN and CMN showed a similar variation against temperature, i.e. had a similar slope, CMN pellets always had higher values than PMN. This is thought to be due to the difference in pellet densities. Although CMN pellets showed around 93% of theoretical density after sintering, mixed oxide pellets gave a value of around 87%. The apparent dielectric constant of the material will

decrease proportional to the porosity, i.e. increase with the volume shrinkage of the sample.[31]

The dielectric loss of PMN pyrochlore showed different behaviour for pellets produced from powders from different routes (Fig. 14(b)). However, the lowest value of dielectric loss is observed for the CMN and it was around 0·0015 at room temperature. Shrout and Swartz[10] produced PMN pyrochlore from mixed oxides and measured its dielectric properties over a temperature range of 4·2 to 400 K. They determined that it has a dielectric constant of ~130 at room temperature with the loss <0·002. These results were in agreement

Fig. 12. Bright-field TEM image of clean grain junctions in CMN pellet sintered 2 h at 1260°C.

Fig. 13. Typical planar defects observed in PMN pyrochlore produced from both mixed oxide and partial oxalate methods (1260°C, 2 h).
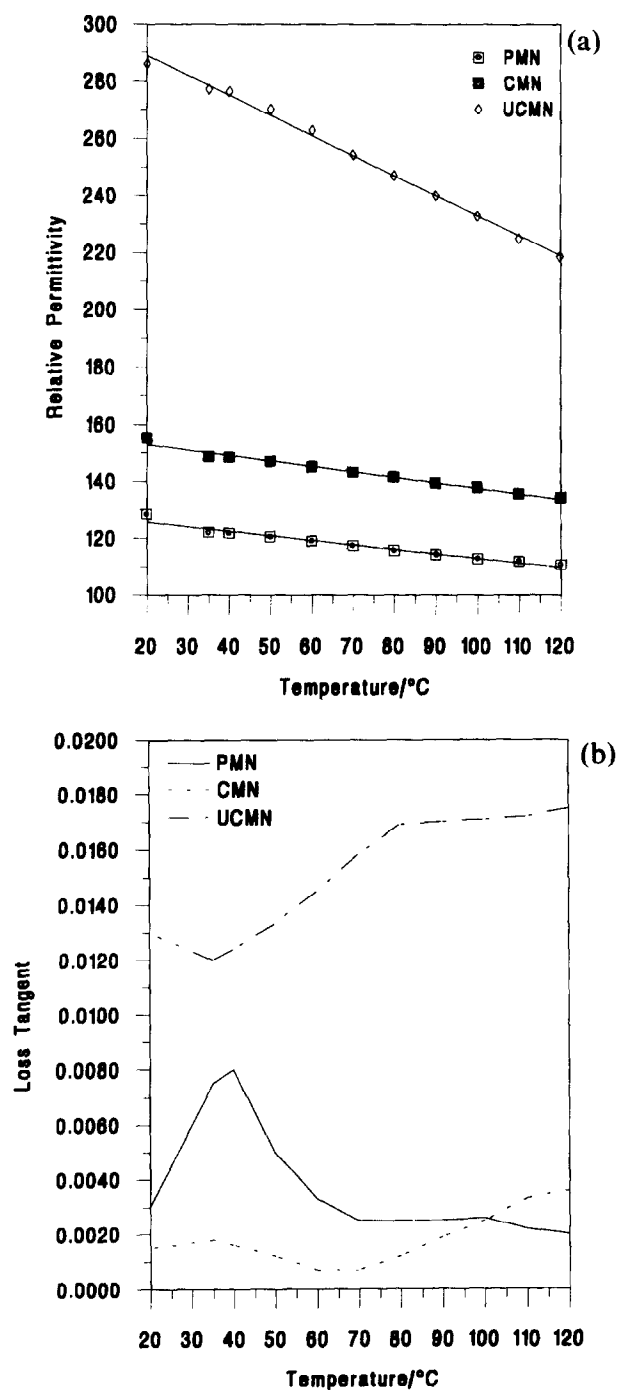

Fig. 14. The temperature dependence of (a) dielectric constant and (b) dielectric loss of PMN pyrochlore produced from mixed oxide (PMN) and partial oxalate (CMN and UCMN) routes and sintered 2 h at 1260°C.

with the results observed in this study, although in CMN pellets higher dielectric constant and lower loss were observed. They also observed that the dielectric constant increased with decreasing temperature with an anomalous peak near 20 K due to a relaxation phenomenon.

4 Conclusions

(1) PMN pyrochlore was produced both from conventional mixed oxides and partial oxalate methods.

(2) Investigations of the reaction sequence to pyrochlore via both methods revealed that formation of pyrochlore is very dependent on the reactivity of MgO. In both methods pyrochlore was not formed by the direct formation of oxides but through some intermediate compounds involving lead niobate pyrochlores due to the low reactivity of refractory MgO. In the mixed oxides method the formation temperature of pyrochlore ($>1000°C$) was higher than that of partial oxalate methods ($>800°C$).

(3) The columbite method affected the reaction sequence of pyrochlore and led to formation of PMN perovskite before pyrochlore indicating that it is an effective way of producing single-phase PMN perovskite.

(4) Although sintered mixed oxide and CMN pellets showed only single-phase pyrochlore, UCMN pellets contained two coexisting phases, pyrochlore and perovskite, and microstructural investigation showed that perovskite grains were distributed generally in clusters between the pyrochlore grains with some Mg-rich phases observed only between perovskite grains.

(5) PMN pyrochlore produced from CMN has the highest dielectric constant (K) and the lowest dielectric loss ($\tan\delta$), $K = 157$ and $\tan\delta = \sim0.0015$ at 20°C.

Acknowledgements

References

1. Ling, H. C., Yan, M. F. & Rhodes, W. W., Phase stability in $Pb(B_{1/2}^{3+}B_{1/2}^{5+})O_3$ and $Pb(B_{1/3}^{2+}B_{2/3}^{5+})O_3$ compositions. *Ferroelectrics*, **89** (1989) 69–80.

2. Smolenskii, G. A. & Agranovskaya, A. I., Dielectric polarization and losses of some complex compounds. *Sov. Phys. Tech. Phys.*, 3 (1958) 1380–1382.

3. Lejeune, M. & Boilot, J. P., Formation mechanism and ceramic process of the ferroelectric perovskites: $Pb(Mg_{1/3}Nb_{2/3})O_3$ and $Pb(Fe_{1/2}Nb_{1/2})O_3$. *Ceramics International*, **8**(3) (1982) 99–103.

4. Lejeune, M. & Boilot, J. P., Influence of ceramic processing on dielectric properties of perovskite type compound: $Pb(Mg_{1/3}Nb_{2/3})O_3$. *Ceramics International*, **9**(4) (1983) 119–122.

5. Swartz, S. L. & Shrout, T. R., Fabrication of perovskite lead magnesium niobate. *Mat. Res. Bull.*, **17**(10) (1982) 1245–1250.

6. Swartz, S. L., Shrout, T. R., Schulze, W. A. & Cross, L. E., Dielectric properties of lead magnesium niobate ceramics. *J. Amer. Ceram. Soc.*, **67**(5) (1984) 311–315.

7. Kang, D. H. & Yoon, H. K., Dielectric properties due to excess PbO and MgO in lead magnesium niobate ceramics. *Ferroelectrics*, **87** (1988) 255–264.

8. Inada, M., Analysis of the formation process of the piezoelectric PCM ceramics. *Japan. Natl Tech. Rept*, **23**(1) (1977) 95–102.

9. Adrianova, I. I., Berezhnoi, A. A., Nefedova, E. V., Pismennyi, V. A., Popov, Y. V. & Skoryakova, K. P., Electro-optical effect in lead magnesium niobate crystals of pyrochlore structure. *Opt. Spectrosc.*, **36**(5) (1974) 547–548.

10. Shrout, T. R. & Swartz, S. L., Dielectric properties of pyrochlore lead magnesium niobate. *Mat. Res. Bull.*, **18**(6) (1983) 663–667.

11. Wakiya, N., Saiki, A., Ishizawa, N., Shinozaki, K. & Mizutani, N., Crystal growth, crystal structure and chemical composition of pyrochlore type compound in lead–magnesium–niobium–oxygen system. *Mat. Res. Bull.*, **28**(2) (1993) 137–143.

12. Wakiya, N., Kim, B. H., Shinozaki, K. & Mizutani, N., Composition range of cubic pyrochlore type compound in lead–magnesium–niobium–oxygen system. *J. Ceram. Soc. Jap.*, **102**(6) (1994) 612–615.

13. Okazaki, K., Advanced technology in electroceramics in Japan. *Am. Ceram. Bull.*, **67**(12) (1988) 1946–1960.

14. Gupta, S. M. & Kulkarni, A. R., Synthesis of perovskite lead magnesium niobate using partial oxalate methods. *Mat. Res. Bull.*, **28**(12) (1993) 1295–1301.

15. Mendelson, M. I., Average grain size in polycrystalline ceramics. *J. Am. Ceram. Soc.*, **52**(8) (1969) 443–446.

16. Brown, H. E., *Lead Oxide Properties and Applications.* International Lead Zinc Research Organisation, New York, 1985.

17. Bouquin, O. & Lejeune, M., Formation of the perovskite phase in the $PbMg_{1/3}Nb_{2/3}O_3$-$PbTiO_3$ system. *J. Am. Ceram. Soc.*, **74**(5) (1991) 1152–1156.

18. Imota, F. & Ilda, H., The formation process of lead magnesio–niobate $Pb(Mg_{1/3}Nb_{2/3})O_3$ in the solid state reaction. *J. Ceram. Soc. Jap.*, **80**(5) (1972) 25–31.

19. Kassarjian, M. P., Newnham, R. E. & Biggers, J. V., Sequence of reactions during calcining of lead-iron niobate dielectric ceramics. *Am. Ceram. Soc. Bull.*, **64**(8) (1985) 1108–1111.

20. Lide, D. R., *Handbook of Chemistry and Physics*, 73rd edn. CRC Press, Boca Raton, FL., 1992–93.

21. Munson, M. J. & Riman, R. E., The chemical and physical properties of metal oxalate calcination reactions. *Ceramic Dielectrics: Composition, Processing and Properties. Ceramic Transactions*, Vol. 8, ed. H. C. Ling & M. F. Yan. Am. Ceram. Soc., Westerville, OH, 1990, pp. 213–220.

22. Mergen, A., Electrical ceramics with the pyrochlore crystal structure in the $ZnO-Bi_2O_3-Sb_2O_3$ and $PbO-MgO-Nb_2O_5$ systems. PhD Thesis, University of Sheffield, UK, 1996.

23. Guha, J. P. & Anderson, H. U., Preparation of perovskite $Pb(Mg_{1/3}Nb_{2/3})O_3$ using $Pb_3Nb_2O_8$ and MgO. *J. Am. Ceram. Soc.*, **69**(11) (1986) C-287–288.

24. Dambekalne, M., Brante, I. & Sternberg, A., The formation process of complex lead-containing niobates. *Ferroelectrics*, **90** (1989) 1–14.

25. Hankey, D. L. & Biggers, J. V., Solid state reactions in the system $PbO-TiO_2-ZrO_2$. *J. Am. Ceram. Soc.*, **64** (1981) C–172–173.

26. Goo, E., Yamamoto, T. & Okazaki, K., Microstructure of lead-magnesium niobate ceramics. *J. Am. Ceram. Soc.*, **69**(8) (1986) C-188–190.

27. Wang, H. C. & Schulze, W. A., The role of excess magnesium oxide or lead oxide in determining the microstructure and properties of lead magnesium niobate. *J. Am. Ceram. Soc.*, **73**(4) (1990) 825–832.

28. Yan, M. F., Ling, H. C. & Rhodes, W. W., Preparation and properties of $PbO-MgO-Nb_2O_5$ ceramics near the $Pb(Mg_{1/3}Nb_{2/3})O_3$ composition. *J. Mater. Res.*, **4**(4) (1989) 930–944.

29. Lee, W. E. & Rainforth, W. M., *Ceramic Microstructures, Property Control by Processing.* Chapman and Hall, London, UK, 1994, p. 176.

30. Lee, W. E., Reaney, I. M. & McCoy, M. A., Planar defects in electroceramics. In *Brit. Ceram. Proc.*, Vol. 55, 1996, pp. 199–212.

31. Ling, H. C., Yan, M. F., Jackson, A. M. & Rhodes, W. W., Effect of PbO evaporation on the composition and dielectric properties of $PbO-MgO-Nb_2O_5$ based dielectrics. *J. Mater. Res.*, **5**(3) (1990) 629–639.